1597 (1969).
[3]F. Tabakin, Phys. Rev. 174, 1208 (1968).
[4]J. S. Levinger, A. H. Lu, and R. Stagat, Phys. Rev. 179, 926 (1969).
[5]F. Perey and B. Buck, Nucl. Phys. 32, 353 (1962); F. G. Perey, in *Direct Interactions and Nuclear Reaction Mechanisms*, edited by E. Clementel and C. Villi (Gordon and Breach, Science Publishers, Inc., New York, 1963), p. 125.
[6]M. Coz, A. D. MacKellar, and L. G. Arnold, Ann. Phys. (N. Y.) 58, 504 (1970).
[7]M. Coz, L. G. Arnold, and A. D. MacKellar, Ann. Phys. (N. Y.) 59, 219 (1970).
[8]H. Fiedeldey, Nucl. Phys. 77, 149 (1966); A96, 463 (1967). The use of two solutions to a nonlocal equation was first suggested by N. Austern, Phys. Rev. 137, B752 (1965).
[9]R. E. Schenter, Nucl. Phys. A94, 408 (1967); A. D. MacKellar, J. F. Reading, and A. K. Kerman, Phys. Rev. C 3, 460 (1971).
[10]A. D. MacKellar and R. E. Schenter, to be published.
[11]G. Breit, Rev. Mod. Phys. 39, 560 (1967); M. H. MacGregor, R. A. Arndt, and R. M. Wright, Phys. Rev. 169, 1128 (1968).
[12]T. Hamada and I. D. Johnston, Nucl. Phys. 34, 383 (1962); K. E. Lassila, M. H. Hull, Jr., H. M. Ruppel, F. A. McDonald, and G. Breit, Phys. Rev. 126, 881 (1962); R. V. Reid, Ann. Phys. (N. Y.) 50, 411 (1968).
[13]Y. Yamaguchi, Phys. Rev. 95, 1628 (1954). We have changed the sign of the Yamaguchi potential so that the potential is attractive (repulsive) in local-potential terminology according to whether λ is negative (positive). The original Yamaguchi potential has a Yukawa form factor $e^{-\beta r}/r$. With our standardization of the s-wave radial equation, the form factor becomes $e^{-\beta r}$.
[14]D. W. L. Sprung and M. K. Srivastava, Nucl. Phys. A139, 605 (1969); D. Gogny, P. Pires, and R. de Tourreil, Phys. Letters 32B, 591 (1970).
[15]M. Bolsterli, Phys. Rev. 182, 1095 (1969).
[16]T. Brady, M. Fuda, E. Harms, J. S. Levinger, and R. Stagat, Phys. Rev. 186, 1069 (1969).
[17]D. W. L. Sprung, lectures delivered at the Herceg Novi Summer School on Nuclear Physics, Herceg Novi, Yugoslavia, 1970 (unpublished).
[18]Z. S. Agranovitch and V. A. Marchenko, *The Inverse Problem of Scattering Theory* (Gordon and Breach, Science Publishers, Inc., New York, 1966).

PHYSICAL REVIEW C VOLUME 3, NUMBER 3 MARCH 1971

Regge Poles and Strong Absorption in Heavy-Ion and α-Nucleus Scattering*

K. W. McVoy†
Argonne National Laboratory, Argonne, Illinois 60439
(Received 28 October 1970)

Regge poles describing shape resonances ("quasimolecular states") are found to play a prominent role in many optical-model scattering amplitudes and appear to be directly related to the Gruhn-Wall "dip" often observed in the reflection coefficient $\eta(l)$. The Blair smooth-cutoff model is generalized to include such a Regge pole and used to fit angular distributions for elastic $^{16}O+^{16}O$ and $\alpha+^{16}O$ scattering, in the 20–30-MeV (c.m.) energy range. It also appears that the smooth-cutoff (strong-absorption) model itself can be interpreted as the result of many overlapping inelastic Regge resonances.

I. INTRODUCTION

A long-standing problem in elastic α-nucleus scattering at energies well above the Coulomb barrier is the strong rise of the angular distributions at backward angles. Although both the optical model with strong absorption and the smooth-cutoff model[1] reproduce the diffractionlike angular distribution in the forward hemisphere, neither has so far been very successful in simultaneously describing the strong, oscillatory backscattering. Bryant and Jarmie[2] have noted that the shape of this backward-angle scattering is strongly reminiscent of the glory effect, which is a grazing-ray phenomenon,[3] and indeed Gruhn and Wall[4] found that a narrow dip superimposed on the smooth-cutoff model at an l value near $l=kR$ aided materially in raising the backward-angle scattering. More significantly, Cowley and Heymann[5] have recently shown that adding a Regge pole at $l\approx kR$ to the smooth-cutoff model permits an impressive fit to their elastic $\alpha+^{16}O$ cross sections over the full angular range.

A direct-channel Regge pole is simply a convenient means of describing resonances in several adjacent l values simultaneously; the fact that the data seem to call for such resonances near $l=kR$ implies considerable transparency of the interaction at the nuclear surface, in spite of its strong absorption near the center. This is reminiscent of the interaction responsible for heavy-ion scattering, for a growing body of opinion[6-8] suggests that it, too, is strongly absorptive at small impact parameters but highly transparent at large

ones. This interpretation is supported by the finding of the Erlangen group[9] that their $^{14}N+^{12}C$ data could be fit with a smooth-cutoff model only by the inclusion of a "dip" at surface l values, in the Gruhn-Wall fashion. Of these various modifications of the smooth-cutoff model, the best-founded is that employing one or more Regge poles, since these poles affect both the amplitude and the phase of the S matrix elements in an appropriately correlated fashion.

Our purpose is, first, to explain how this is accomplished by examining single-particle Regge poles, such as those which occur naturally in any optical-model calculation, and second to suggest a slight modification of the Regge representation used by Cowley and Heymann. This alternate form (a product rather than a sum) has the double advantage of introducing the Gruhn-Wall dip in an easily-controlled manner, and of being manifestly unitary. Finally we show that a careful examination of the strong absorption described by optical potentials suggests that it can be interpreted as due entirely to overlapping Regge resonances, i.e., that diffraction can be viewed as a resonance phenomenon.

II. PRODUCT REGGE REPRESENTATION

The customary smooth-cutoff representation, for the l dependence of the "nuclear" diagonal S matrix elements in the entrance channel of interest, is generally taken to have the form[10]

$$S_l=[1+e^{-i\alpha}e^{(L-l)/\Delta}]^{-1}\equiv B(l), \tag{1}$$

in terms of which the scattering amplitude, including Coulomb effects, is given by

$$f(\theta)=f_C(\theta)+\frac{1}{2ik}\sum(2l+1)e^{2i\sigma_l}(S_l-1)P_l(\cos\theta). \tag{2}$$

Here $f_C(\theta)$ is the point-Coulomb amplitude,

$$e^{2i\sigma_l}=\Gamma(l+1+i\eta)/\Gamma(l+1-i\eta),$$

and

$$\eta=ZZ'e^2/\hbar v.$$

If we call

$$\eta_l\equiv|S_l| \tag{3}$$

the "reflection coefficient," then the reflection coefficient given by Eq. (1) has the usual smooth S-shaped rise to unity as a function of l, centered at L, with width Δ.

The modification we wish to suggest employs this $B(l)$ as a "background." It is multiplied by a single Regge-pole factor (i.e., a Breit-Wigner approximation in l) and the result, in its simplest version, can be written in either of the equivalent forms

$$S(l)=B(l)\left[\frac{l-L_0-iz(l)}{l-L_0-ip(l)}\right] \tag{4a}$$

$$=B(l)\left[1+i\frac{D(l)}{l-L_0-i\hat{\Gamma}(l)/2}\right]. \tag{4b}$$

From (4b) it is clear that the extra factor describes a resonance in l, centered at L_0 with total l width $\hat{\Gamma}$.[11] In analogy to the energy-dependent widths of the usual Breit-Wigner approximation, D and Γ are themselves slowly l dependent; as explained below, they must vanish exponentially as $l\to\infty$. It is reasonable that they should do so at the same rate as $[B(l)-1]$, so we shall adopt for them the convenient forms

$$D(l)=D/[1+e^{(l-L)/\Delta}], \tag{5a}$$

$$\hat{\Gamma}(l)=\hat{\Gamma}/[1+e^{(l-L)/\Delta}], \tag{5b}$$

in which D and $\hat{\Gamma}$ play the role of "reduced widths." The $z(l)$ and $p(l)$ of Eq. (4a) obviously have the same exponential dependence as Eq. (5), with the reduced p (pole) and z (zero) parameters given by

$$p=\tfrac{1}{2}\hat{\Gamma} \tag{6}$$

and

$$z=\tfrac{1}{2}\hat{\Gamma}-D. \tag{7}$$

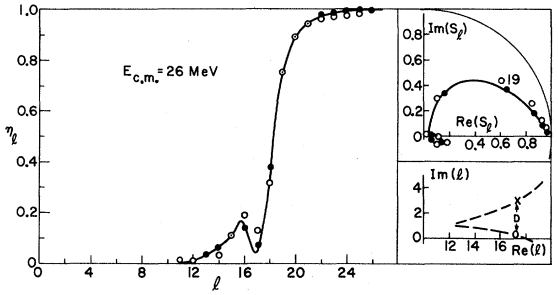

FIG. 1. A partial-wave analysis provided by the Regge-pole-plus-smooth-cutoff model of Eq. (4). The parameter values of the model are given in Table I, and were obtained by fitting the model to an angular distribution generated by the optical potential of Eqs. (9a) and (9b), which has been used to fit $^{16}O+^{16}O$ elastic scattering. The plot in the upper right-hand corner is the first quadrant of the Argand diagram, on which the complex S-matrix elements from the optical potential are indicated by open circles and those of the model by solid dots. (Where the two coincide, the dot is within the circle.) The curve is drawn through the dots and proceeds from the $l=14$ dot near the origin to the $l=22$ dot near (1, 0); the $l=19$ position is indicated along the curve. The left-hand plot shows $\eta(l)=|S(l)|$ vs l with the same conventions, and the lower right-hand plot shows the positions of the complex L_0+ip and L_0+iz (the approximate pole and zero positions predicted by the model) in the complex l plane.

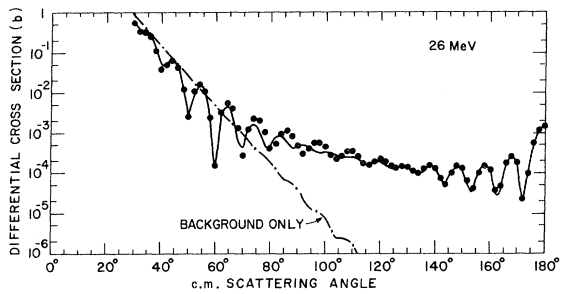

FIG. 2. Angular-distribution fit corresponding to Fig. 1. The dots are the "data" generated by the optical potential, and the solid curve is the best six-parameter fit to it with the model of Eq. (4). The oscillatory rise of the cross section at backward angles (the glory effect) is entirely due to the influence of the Regge pole.

The modified smooth-cutoff model given by Eq. (4) thus contains six real parameters: L, Δ, and α for the background and L_0, $\hat{\Gamma}$, and D for the Regge resonance. Since $|B| \leq 1$, the unitarity condition will certainly be satisfied if $0 \leq |z| \leq p$, or equivalently if $0 \leq D \leq \hat{\Gamma}$. The significance of $z(l)$ and $p(l)$, incidentally, can best be appreciated from the fact that if their l dependence is sufficiently slow, $S(l)$ will have a pole (Regge pole) at $l \approx L_0 + ip(L_0)$, and a zero at $l \approx L_0 + iz(L_0)$; this indeed appears to be the case for the scattering systems considered so far. The pole must always be in the upper half of the l plane, and the zero is in the lower half if $D > \frac{1}{2}\hat{\Gamma}$.

Although the explanation of the physical significance of Eq. (4) will be postponed to a later section, its practical effects can be seen in the reflection coefficients of Fig. 1, in which a Regge zero at a complex l near $l = 17$ has produced a sharp dip in the curve, and a consequent effective steepening of its rise toward 1. The corresponding angular distribution, Fig. 2, exhibits the characteristic backward-angle glory oscillations, which are seen to vanish entirely if the pole-zero factor is removed from the model.

The physical significance of these effects will become somewhat clearer in the following sections, which investigate some of the Regge poles that occur in optical-potential scattering amplitudes.

III. REGGE POLES AND ZEROS IN OPTICAL-MODEL CALCULATIONS

A. Poles and Spectroscopy

A Regge pole describes a sequence of energy levels which are distinguished by different values of the angular momentum quantum number J, but are related by a common value of a second quantum number. Examples from nuclear physics are (1) a rotational band of states (related by the intrinsic angular momentum K), and (2) a Regge trajectory for a potential well, i.e., all the states of the well which have the same value of the radial quantum number n. These single-particle states are the ones which can occur in optical calculations, and indeed a survey of many such calculations shows that all nuclear optical potentials except those corresponding to extremely strong absorption have scattering amplitudes which exhibit prominent Regge poles. These poles can often be most clearly seen as resonance peaks in the l dependence of the transmission coefficient $T(l,E) = 1 - |S(l,E)|^2$ at fixed E. A typical example is shown in the insert of Fig. 3, which exhibits six such l resonances labeled by their radial quantum numbers n.

Several years ago similar l oscillations in the reflection coefficients for α-nucleus scattering were noted by Austern,[12] who interpreted them as the result of an interference between waves reflected from the "inner" and "outer" parts of the centrifugal potential in the neighborhood of the barrier. The point we wish to add is simply that the "destructive" interferences, those which produce minima in $\eta(l)$, correspond to single-particle resonances.

These resonances seen in the l dependence of the scattering amplitude are of course the same as those seen in its E dependence. The relation between the two is perhaps best understood by noting that the radial Schrödinger equation for a spherically symmetric potential can be solved, subject to the usual $r = 0$ boundary condition, for arbitrary real or complex E and l, thus defining the S-matrix elements $S_l(E) \equiv S(l,E)$ throughout the complex E and l planes. As a function of these two variables it has a pole associated with each bound or resonant state of the potential, the pole occurring *at* the appropriate physical (l,E) combination in the case of a bound state, and near it in the case of a resonance.

Passing near such a pole along either the real l axis or the real E axis can produce a maximum in the transmission coefficient.[13] This is illustrated clearly in Fig. 3,[14] which shows a number of resonance maxima as a function of E for fixed l, together with an orthogonal "slice" at 16 MeV showing the same resonances as a function of l for fixed E.

These resonances occur at the energies $E_{n,l}$, which of course increase both with increasing n (radial energy) and with increasing l (rotational energy). Thus, e.g., the $2h$ level occurs for this potential at 12.8 MeV, while the $2i$ level appears at 14 MeV. The successive reappearances of the $n = 2$ state for higher and higher l values are called "Regge recurrences," for $n = 2$, and this entire sequence of l values, for fixed n and increasing

E, describes the $n=2$ Regge trajectory of the potential.

This figure includes the $n=0$, 1, 2, 3, 4, and 5 trajectories and illustrates the important fact that each appears to "end" at a maximum l value, at which the resonance becomes so broad it merges into the background. This is because these are

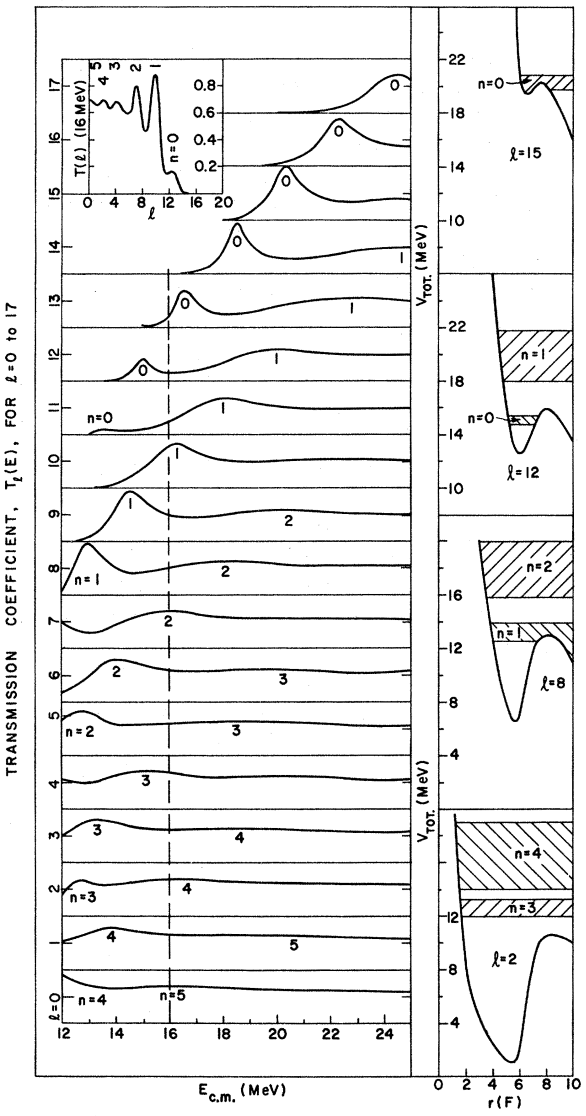

FIG. 3. Optical-potential transmission coefficients vs $E_{c.m.}$, for $l=0$ to 17, showing resonance maxima which are labeled by their radial quantum numbers. The potential is that of Eqs. (9a) and (9b), with $W_0 \equiv 0.5$ MeV, $R_2=6.9$, $a_2=0.49$. The locus of maxima for a fixed n gives a Chew-Frautschi plot for the corresponding Regge pole. The same data are plotted vs l in the insert for $E=16$ MeV, showing how the five Regge poles present cause peaks in T as a function of l. The potential curves show $-V(r)+V_{\text{Coulomb}}+\hbar^2 l(l+1)2\mu r^2$ for several l values, indicating how resonances rise out of the potential "pocket" as l increases and the pocket fills in.

potential resonances, due entirely to the centrifugal (plus Coulomb) barrier, the height of which increases with l, so that each higher-l recurrence of a resonance along a Regge trajectory is a resonance behind a higher potential barrier. Both the barrier height and the resonance energy increase with increasing l, however, and the resonance energy necessarily moves up faster than the barrier[15]; consequently at some l the resonance will rise above the barrier, broaden, and vanish into the background. As Fig. 3 indicates, this final disappearance generally seems to occur for this potential only after the resonance has risen several MeV above the top of the corresponding barrier.

For a given l, the higher-n states of course lie higher in energy than the low-n ones (cf. $n=0$ and 1 for $l=12$), and so rise above the barrier first as l increases; in Fig. 3, e.g., this happens at $l=1$ and $E=20$ MeV for the $n=5$ state, but not until $l=10$ and $E=23$ MeV for the $n=2$ state.

The levels indicated in the 16 MeV insert in Fig. 3 ($5s$, $4d$, $3g$, etc.) are just the levels of this potential which are (within the leeway allowed by their widths) degenerate at 16 MeV. Since they all have the same energy but are caused by potential barriers which decrease with decreasing l, the lower-l (higher-n) states will always have broader widths, both in E and in l, than the higher-l ones. Since their l spacings also decrease with decreasing l, the low-l states exhibit a much higher degree of overlap (in l) than do the high-l ones. It is clearly just this increased overlap which causes $T(l,E)$ to rise to a larger average value (indicating stronger absorption) at low l than at high l, a significant point to which we shall return below.

The energy at which the "last" ($n=0$) resonance rises above its barrier is a very important one, for it is generally just a few MeV above the energy at which the increase in l fills in the "resonance pocket" behind the barrier altogether. Obviously resonances cannot occur substantially above this energy, which we shall call $E_{\text{fill in}}$. $E_{\text{fill in}}$ is thus a fundamental characteristic of the potential, marking the division between its resonance and nonresonance energy regions. $E_{\text{fill in}}$ for the potential of Fig. 3 is about 17 MeV.

B. Regge Zeros and Strong Absorption

In a $T(E)$ curve like those shown in Fig. 3, a resonant E or l is normally marked by that point on the curve at which $T(l,E)$ reaches a maximum. This is a point at which the reflection coefficient $\eta(l,E)$ reaches a minimum, and this minimum, just as in Fig. 1, will be determined by a nearby zero of $S(l,E)$: Although a resonance is normally associated with a Regge pole, the reflection coeffi-

cient is more strongly affected, at an inelastic resonance, by the associated Regge zero.

The importance of this zero is made even clearer by the observation that along every Regge trajectory shown in Fig. 3, there is one (l, E) point at which $T(l, E)$ rises exactly to $T=1$. Since this can only happen if a "dip" in $\eta(l)$ reaches $\eta=0$, it can alternately be described as an (l, E) point at which a zero of $S(l, E)$ occurs for *real* l and E (though in general not for an integral l value). It follows from Eq. (4) that this can happen only if

$$D=\tfrac{1}{2}\hat{\Gamma}. \tag{8}$$

The energy and l at which this occurs will be determined largely by the depth of the imaginary part of the optical potential. As E and l increase along a Regge trajectory, the resonance rises above its barrier and increases its elastic width (proportional to D) until eventually $D=\hat{\Gamma}/2$, and T rises to unity. For lower values of l and E along the trajectory, $D<\hat{\Gamma}/2$ and the resonance is predominantly inelastic, while for higher values, $D>\hat{\Gamma}/2$ and it is predominantly elastic. For the present potential the crossover is seen to occur for resonance energies which are actually somewhat above the corresponding barrier energy; for imaginary potentials deeper than 0.5 MeV, it will occur at higher energies still, where the resonances become extremely broad.[16]

The relationship between Regge zeros and strong absorption can be seen in Fig. 4, which displays the reflection coefficients, transmission, coefficients, and Argand diagrams of a set of S-matrix elements, all as a function of l for constant E, for ^{16}O potentials with imaginary well depths of 1, 2, 3, and 5 MeV. The radial quantum numbers of the resonances are again included, labeling peaks in the transmission coefficients and the corresponding dips in the reflection coefficients.

The multiple loops in the Argand diagram are best understood by first considering the Argand diagram of Fig. 5, on which Im$S(l)$ is plotted vs Re$S(l)$ for the case of an isolated Regge pole with no background, i.e., Eq. (4) with $B(l)\equiv 1$. In this case the complex number S travels around a "resonance circle" (beginning and ending at +1) as l increases from below L_0 to above L_0. The circle is traversed in the clockwise or decreasing-phase direction, corresponding to the fact that an elastic

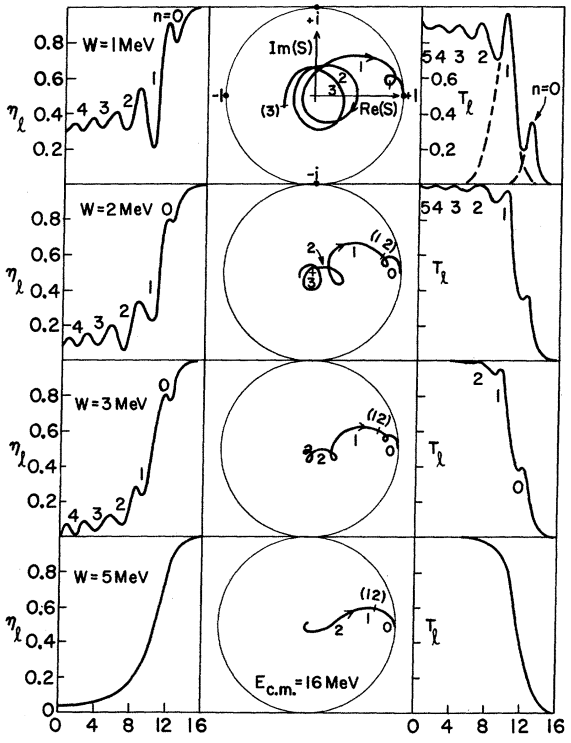

FIG. 4. An indication of how overlapping Regge resonances can result in strong absorption. All curves are calculated with the optical potential of Fig. 3, with $W=1$, 2, 3, or 5 MeV. The left and right graphs are of $\eta(l)$ and $T(l)=1-[\eta(l)]^2$, and the center one shows the corresponding Argand diagrams. The radial quantum numbers indicate the positions of the resonances, and the position of $S(12)$ is indicated by (12) on the Argand plots. The shapes of the $n=0$ and $n=1$ resonances in $T(l)$ are suggested for $W=1$ MeV; it is their strong overlap for $W\geq 5$ that produces the smooth cutoff of $T(l)$ and $\eta(l)$ in that strong absorption limit.

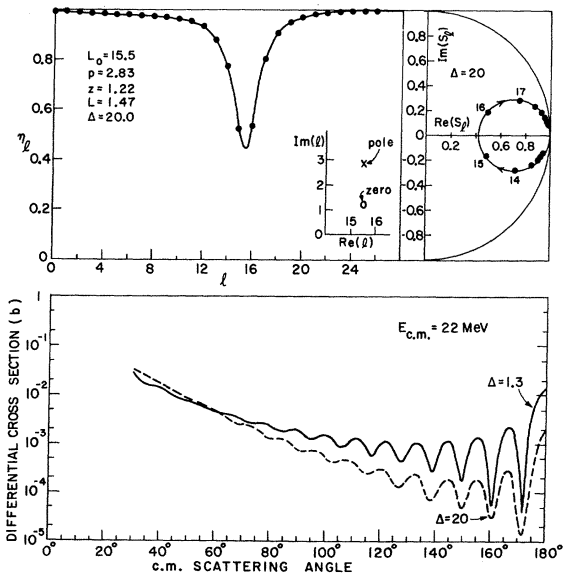

FIG. 5. $\eta(l)$, Argand diagram, pole and zero positions, and angular distribution for a single (modified) Regge pole at 22 MeV for the ^{16}O+^{16}O system (without Coulomb or symmetrization effects). The dashed curve is for $\Delta=20$ [i.e., the Δ of Eq. (5)], and the solid curve for $\Delta=1.3$, the best-fit value used in Fig. 6.

phase shift $\delta(l)$ *decreases* by π as l increases past a Regge pole.[3] This behavior, opposite to what occurs as a function of E, is due to the fact that the Regge pole lies above the real axis in the complex l plane, while the energy pole lies below it in the E plane. This also explains the unconventional signs which occur in Eq. (4b).

The size of the resonance circle is directly related to the zero position. If the resonance is elastic, the resonance circle is the unit circle; the unitarity condition $S(l)S^*(l) \equiv 1$ then requires that any pole at $L_0 + i\hat{\Gamma}/2$ be accompanied by a zero at the complex-conjugate position $L_0 - i\hat{\Gamma}/2$. If the Regge resonance is inelastic (as it will be, e.g., if the optical potential is complex), its zero is closer to the real l axis than is the pole. The resonance circle then has a radius $\rho = \hat{\Gamma}_{el}/\hat{\Gamma} \approx |B(L_0)|D/\hat{\Gamma}$, and will encircle the origin if $D > \hat{\Gamma}/2$, and will not encircle the origin if $D < \hat{\Gamma}/2$. According to Eq. (7) the zero of $S(l)$ will lie in the lower half plane in the first case (resonance predominantly elastic, as the high-energy end of a Regge trajectory), and in the upper half plane, near the pole, in the second case (resonance predominantly inelastic, as at the low-energy end of a Regge trajectory). In the intermediate case, $D = \hat{\Gamma}/2$, the zero occurs for real l, and consequently the Argand-diagram $S(l)$ curve passes directly through the origin.

Returning to the Argand diagram for $W = 1$ MeV in Fig. 4, we see that it contains a number of resonance circles, which are a bit difficult to disentangle because their resonances are overlapping in l, as the transmission-coefficient graph shows. The $n = 2$ and $n = 3$ circles are fairly simple and are seen to correspond to predominantly elastic resonances, since they encircle the origin. The $n = 1$ circle does, as well, but only a little more than half of it is present because the wings of this resonance are overlapped by the $n = 0$ and $n = 2$ resonances. Similarly, only a small fraction of the $n = 0$ circle is visible, for it is seriously overlapped on the low-l side by the $n = 1$ resonance, which causes a small loop at about $l = 12$ to be inserted between the two.

If W is increased to 2 MeV, the resonances become more inelastic and now both the $n = 0$ and $n = 1$ states have $D < \hat{\Gamma}/2$, with "circles" which fall short of the origin. In addition, all resonances are broadened and overlap more; only the very tops of the $n = 2$, 3, 4, and 5 peaks are distinguishable in the transmission-coefficient curve, and only the high-l sides of the $n = 0$ and $n = 1$ states. Correspondingly only the high-l sides of their resonance circles occur in the Argand diagram.

With $W = 3$ MeV almost all resonance circles have become disengaged from the origin and only a small segment of each one is visible between its overlapping neighbors. More importantly, the low-l peaks overlap so strongly in the transmission-coefficient curve that below $l = 7$, $T(l)$ is almost identically unity. In the same way, the overlapping "inverted peaks" in the reflection-coefficient curve hold $\eta(l)$ down to very small values for $l < 7$: *Overlapping inelastic Regge resonances produce strong absorption.*

Finally, when $W = 5$ MeV the overlap is complete, and $\eta(l)$ exhibits the usual smooth rise characteristic of strong absorption. Similarly, in the Argand diagram even the loops separating the segments of the contributing resonance circles have become invisibly small, and these segments appear to join smoothly to produce the nearly real $S(l)$ curve customarily associated with strong absorption. It is in this sense that it appears legitimate to regard the strong-absorption limit, with its diffractive angular distributions, as an overlapping-inelastic-resonance phenomenon, with the shoulder of the $\eta(l)$ curve built up of the tails of many overlapping states.

Although this interpretation might at first sight seem to be at variance with the picture of diffraction as a "prompt" process, it is not. Low-l Regge poles in a traditional flat-bottomed optical potential are spaced two units apart in l, so they will overlap only when their l widths are greater than about 2. A simple estimate of the energy-widths of the corresponding states, based on the Regge equation of Ref. 15, indicates that resonances this broad have lifetimes comparable with the free-particle transit time across the nucleus. Consequently the strong absorption given by their overlap does, in fact, describe a prompt process.

IV. APPLICATIONS AND EXTENSIONS OF THE MODEL

A. True and Modified Regge Poles

The angular distribution produced by a single Regge pole in $S(l)$ is proportional to $|P_L(-\cos\theta)|^2$, where $L = L_0 + i\hat{\Gamma}/2$ is the complex pole position. If $\hat{\Gamma} \ll L_0$, this oscillates at backward angles very much like $|P_{L_0}(\cos\theta)|^2$ (with its zeros filled in), but at $\theta = 0$ it diverges logarithmically for any nonintegral L.

This physically unacceptable behavior is related to the divergence of the partial-wave expansion of $P_L(-\cos\theta)$ at $\theta = 0$ which occurs because a one-pole $S(l)$ approaches unity for large l only very slowly, as l^{-1}, whereas for any interaction with an exponential tail in r, such as the Woods-Saxon potential, $(S - 1)$ must vanish exponentially in l as $l \to \infty$. The l-dependent widths introduced in Eq. (5) ensure this exponential behavior and remove the

$\theta = 0$ divergence,[17] much in the manner of the Khuri-Jones representation.[18]

It is difficult to compute a true Regge-pole angular distribution using Eq. (4) with $B \equiv 1$ and $\Delta = \infty$, because of the large number of partial waves which contribute, but a reasonable approximation can be achieved by using a large but finite Δ. Figure 5 shows the result for $\Delta = 20$, using the λ for 22-MeV (c.m.) ^{16}O-^{16}O scattering; it is compared with the more realistic $\Delta = 1.3$ angular distribution, which rises less steeply at small angles, as expected. Both exhibit the characteristic glory-type oscillations near 180°.

B. Heavy-Ion Scattering

Although it seems likely that heavy-ion angular distributions will exhibit Regge-pole effects, these effects may be difficult to identify because they appear most distinctively at backward angles, where they can be obscured by competition from zero-Q transfer reactions.[19] Only collisions between identical nuclei are free of this ambiguity,

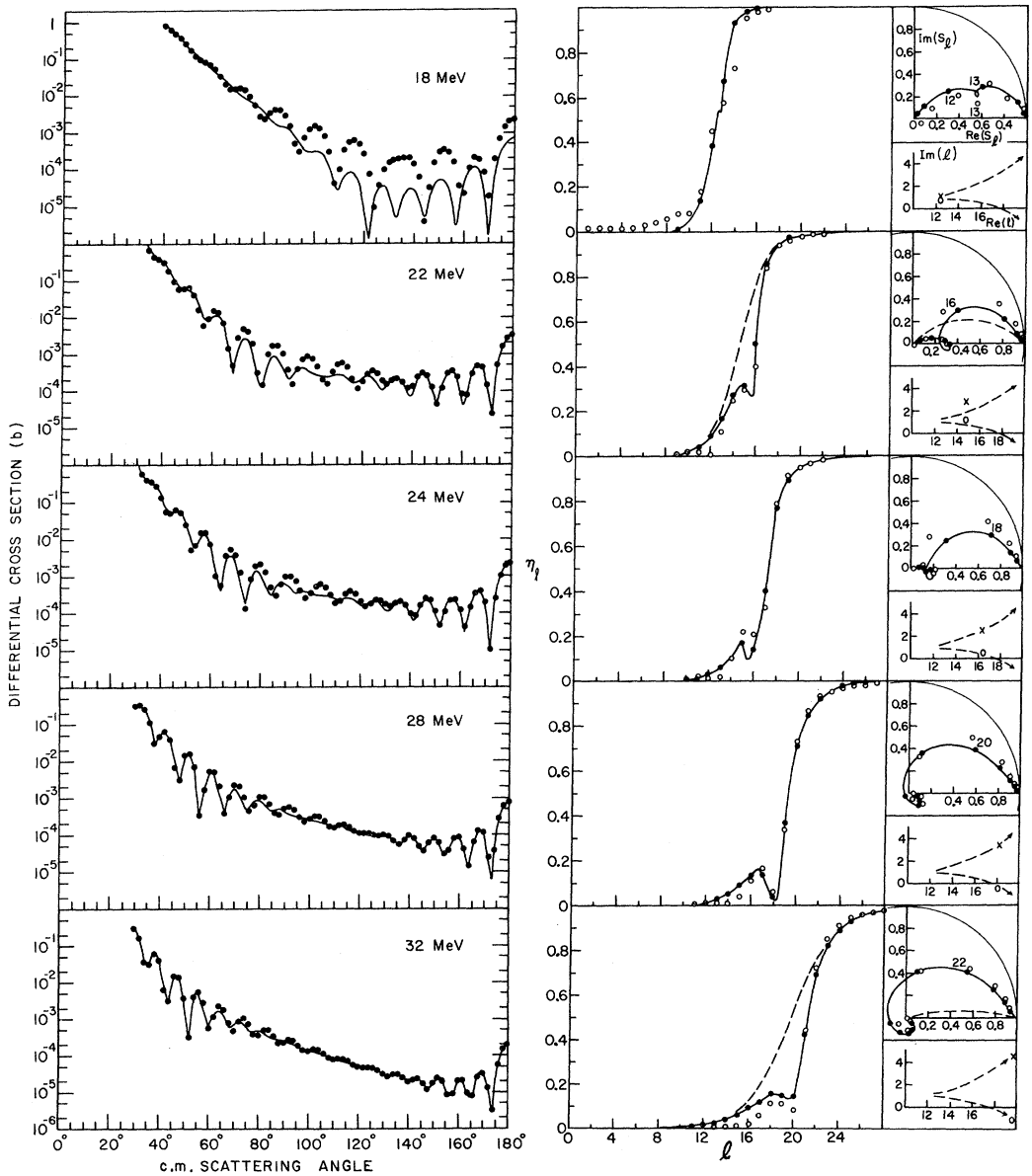

FIG. 6. Fits of the model of Eq. (4) to the ^{16}O+^{16}O optical-potential cross section (unsymmetrized). The potential is that of Eq. (10), and the notation for the partial-wave plots is as in Fig. 1, circles for the optical-potential "data," and dots for the model predictions. The position of one of the S_ℓ's is indicated by the corresponding ℓ value on each Argand plot.

but in this case the backward-angle details are obscured by the symmetry of the angular distribution about 90°. Still another concern is the occurrence of compound-nucleus structure in some heavy-ion excitation functions, which cannot be described by Regge poles if they are, as we suspect, of the single-cluster type.

As a means of avoiding these difficulties until more detailed data become available, we have chosen to apply the cutoff-plus-pole model not directly to experimental angular distributions, but to angular distributions computed from an optical potential which has itself been used to fit experimental heavy-ion data. This not only ensures that compound-nucleus effects have been averaged out, but also permits a verification that any fits achieved are not spurious, since the resulting S_l's can be compared directly with those of the original optical potential.

The potential we have to generate these synthetic data is one of those used by Maher, Siemssen, and Sachs[20] to fit elastic $^{16}O+^{16}O$ cross sections.[6,21] It is a volume-absorption potential, $-V(r)-iW(r)$, with

$$V(r)=V_0[1+e^{(r-R_1)/a_1}]^{-1}, \tag{9a}$$

$$W(r)=W_0(E)[1+e^{(r-R_2)/a_2}]^{-1}, \tag{9b}$$

and

$$V_0=17 \text{ MeV}, \quad R_1=6.8 \text{ fm}, \quad a_1=0.49 \text{ fm},$$

$$W_0(E)=(-17.2+1.86E_{\text{c.m.}}) \text{ MeV},$$

$$R_2=4.17 \text{ fm}, \quad a_2=0.805 \text{ fm}.$$

It differs from the original 17-MeV potential[6] in having much stronger absorption at small radii for $E_{\text{c.m.}}>10$ MeV. Although the scattering amplitude must, of course, be symmetrized to fit the $^{16}O+^{16}O$ data, we have used it without symmetrization in order to see the details of the large-angle scattering.

Figure 6 shows a sequence of fits to these synthetic data, obtained with the $S(l)$ parametrization of Eq. (4) by searching the angular distributions with the multiparameter search code GASIMP provided by the University of Wisconsin Computing Center. The resulting model parameters are listed in Table I. Such a search is in essence a partial-wave analysis within the constraints of the model; the degree of success achieved in finding the correct S-matrix elements (or complex phase shifts) is indicated in the diagrams on the right of this figure. The one-pole-plus cutoff model is seen to provide a very adequate representation of the scattering amplitude above 18 MeV.

TABLE I. Model parameters corresponding to the fits shown in Fig. 6.

$E_{\text{c.m.}}$ (MeV)	$\hat{\Gamma}$	D	L_0	L	Δ	α
18	2.32	0.16	12.8	12.5	0.804	1.14
22	5.64	0.60	15.5	14.7	1.31	0.775
24	5.04	1.99	16.3	16.3	1.32	0.700
26	6.04	2.76	17.2	17.3	1.40	0.722
28	7.02	3.54	18.1	18.1	1.62	0.526
30	8.30	4.17	18.9	19.0	1.62	0.733
32	9.12	5.69	19.7	19.7	1.96	0.251

The influence of the pole-zero factor shows up as a "Gruhn-Wall dip" in $\eta(l)$, or equivalently as a half circle in the Argand diagram, which is terminated on the low-l end by a loop [corresponding to the $\eta(l)$ dip] where the $B(l)$ factor becomes very small. For comparison, the dashed curves on the 22- and 32-MeV diagrams indicate the "background-only" results, obtained by removing the pole-zero factor from Eq. (4); these results, of course, exhibit no dip.

The physical significance of the angular-distribution fits is best seen in Fig. 7, which displays the angular distributions that would result in each case by using (a) the smooth-cutoff background only, $S(l)=B(l)$ (including the Coulomb amplitude and Coulomb phases σ_l), and (b) the pole-zero factor only $[B(l)\equiv 1]$, with no Coulomb effects.

At 18 MeV the (poor quality) fit follows the pattern found by Cowley and Heymann[5] in the $\alpha+^{16}O$ case. The diffuseness parameter Δ of the background is sufficiently small that the smooth-cutoff model by itself provides normal diffraction minima. The pole contribution is very small (the zero nearly coincides with the pole as Fig. 6 shows), but it suffices to shift the positions of the foreward minima and to raise the backward cross section by an order of magnitude.

In all other cases, on the other hand, the search procedure resulted in a Δ sufficiently large (1.3 or greater) that the smooth-cutoff model alone produced no angular maxima or minima except at cross-section values below 10^{-8} b, where they are too small to contribute significantly. In all these cases the background-only pole-only cross sections intersect at angles varying from 20 to 60°. The forward-hemisphere "diffraction" oscillations in the model cross section occur at immediately subsequent angles and appear to result from an "interference" between these two contributions.[22] The 180° cross section, on the other hand, is entirely due to the Regge pole, being typically 10^6 times larger than the 180° background-only cross section. Thus it appears correct to identify the backward-angle oscillations in these cross sections with the glory effect,[2,3] and the forward-angle oscillations with background-resonance inter-

ference. Diffraction in the traditional (nonresonant) sense seems to play no significant role.

The forward-hemisphere interference oscillations generally exhibit a deepest minimum, which occurs where the destructive interference between the resonant and background contributions is strongest. Because the background amplitude falls off with angle much more steeply than does the resonant one, the position of this deepest minimum can easily be moved to more forward angles simply by increasing D, the "strength" of the pole term, or by decreasing the strength of the background term. Both of these changes occur simultaneously as the energy is increased (the importance of the "background" decreasing as the Coulomb scattering decreases), and indeed the deepest forward minimum moves from 80° at 22 MeV to 50° at 32 MeV. Incidentally, because the angular distribution is so dominated by a single pole in this region, the angular spacing between successive minima is determined by the L_0 of the pole as $180°/(L_0+1)$.

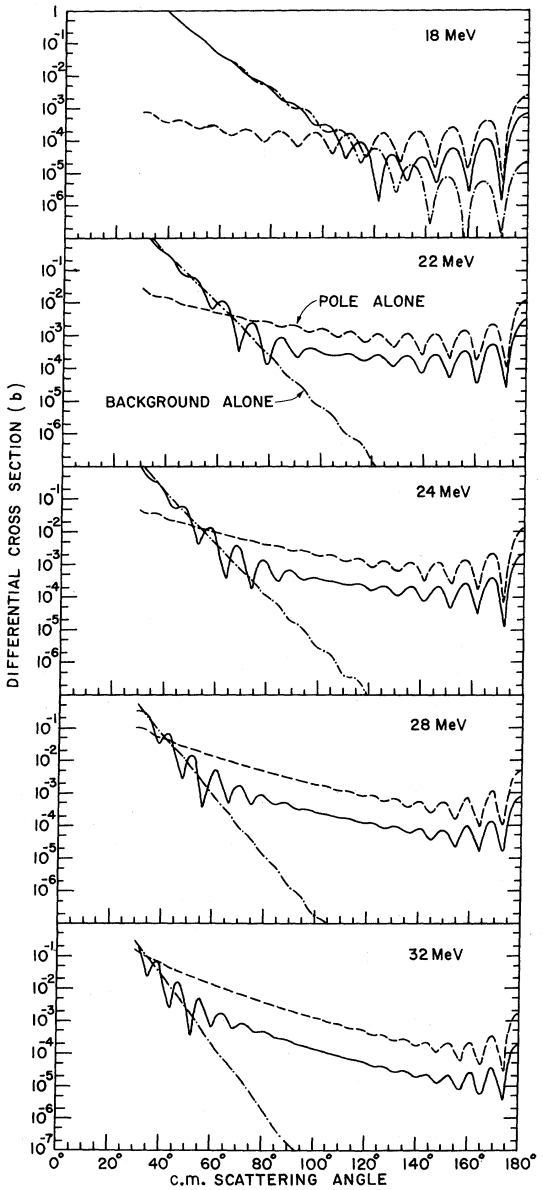

FIG. 7. Pole-plus-background decomposition of angular-distribution fits of Fig. 6. The solid curve is a repeat of the best-fit model curve from Fig. 6. The dash-dot curve (background only) is the angular distribution given by these same model parameters (including Coulomb effects) if the pole-zero factor of Eq. (4) is removed, and the dashed curve is the angular distribution given by the pole-zero factor alone (without Coulomb effects).

A particularly fascinating feature of these angular distributions (which vanishes from sight if they are symmetrized) is the "smooth section" near the middle angles, which begins to appear near 125° at 26 MeV, and has broadened to cover the region between 90 and 140° by 32 MeV. Its physical significance is not yet clear, but the overwhelming importance of the Regge pole in the 32-MeV Argand diagram shows it to be a one-Regge-pole phenomenon.[23] It is found to occur in all optical calculations which utilize the real part of this potential, with or without Coulomb effects and with or without absorption. In all cases it commences about 10 MeV above $E_{\text{fill in}}$ (which can be changed drastically by changing the Coulomb potential or the surface thickness a_1) and continues "expanding" up to at least $E_{\text{c.m.}}=70$ MeV.[24] Whatever its physical meaning, this "smooth section" may prove to be the most easily recognized signature of a one-Regge-pole-plus-background partial-wave decomposition.

The energy dependence of the model parameters, and especially of the $\eta(l)$ curve, is of considerable physical significance, and can be directly related to Figs. 3 and 4. Extrapolation from Fig. 3 shows that the Regge pole being "followed" in the 20–30 MeV energy range is the "last" or $n=0$ one, which occurs at the highest l values. Its pole and zero positions are not far from (L_0+ip) and (L_0+iz), and the trajectories followed by these numbers in the complex l plane as the energy increases are indicated at the right of Fig. 6.[25] At higher energies they will recede vertically from the real axis and "turn back" to the left, corresponding to the broadening and vanishing of this highest-energy resonance into the background, as in Fig. 3. It is only because this occurs at lower energies for all the higher-n resonances that the $n=0$ resonance occurs in isolation above 22 MeV and permits a one-pole model to work there. It is clear from the dip in the "data" $\eta(l)$ curve at 18 MeV that the $n=1$ resonance also exerts a substantial

influence at that energy, which is why a one-pole model is incapable of fitting the angular distribution there. As far as single-cluster Regge poles are concerned, *a one-pole representation is likely to be adequate only if* $E_{\text{c.m.}}$ *is well above* E_{fillin}.

The l value at which $|B(l)| = \frac{1}{2}$ (call it $l_{1/2}$), which is approximately the l at which the barrier maximum equals the scattering energy, increases with scattering energy roughly as $E^{1/2}$. The L_0 of a pole increases less rapidly with E; this is merely a restatement of the previously-noted fact that as l increases, resonance energies increase faster than the barrier energy. Thus as the smooth-cutoff "shoulder" in $\eta(l)$ moves to the right with increasing energy, it overtakes the Regge poles one by one, which appear to "slide down the hill" as Fig. 6 shows. At some point in the process the dip in $\eta(l)$ extends down to $\eta = 0$, namely at that energy at which the Regge zero crosses the real l axis, which is where $D = \hat{\Gamma}/2$. Thereafter the dip in $\eta(l)$ fills in and drops to an l below $l_{1/2}$, where it joins and overlaps the higher-n dips to become part of the strong-absorption background. Note, incidentally, that the resonance becomes more elastic as the energy increases.

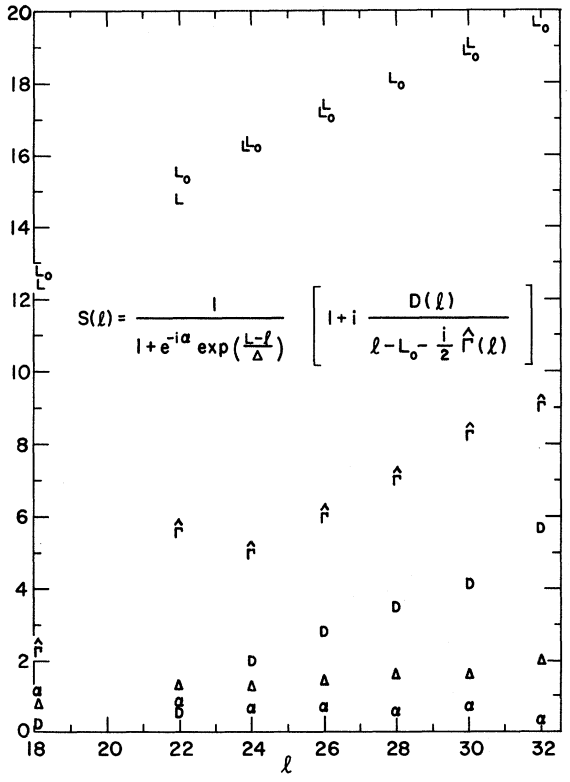

FIG. 8. Energy dependence of the model parameters of Table I. The value of each parameter is indicated by the appropriate symbol; where L and L_0 come at the same point, only L_0 is plotted. No fit was obtained at 20 MeV.

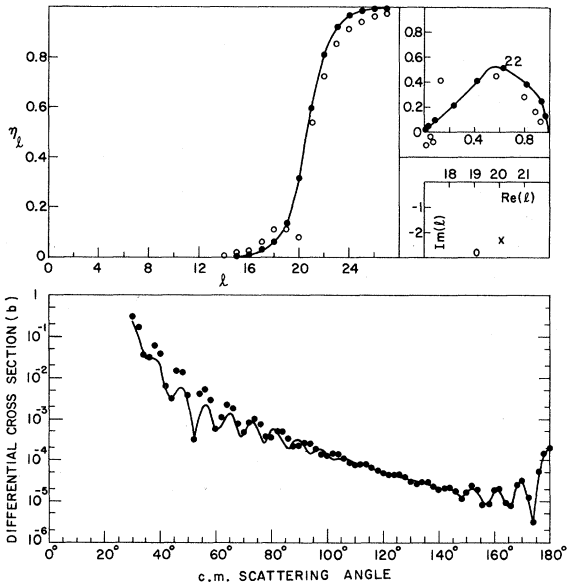

FIG. 9. Spurious fit to the 32-MeV synthetic data of Fig. 6. The model parameters are $\hat{\Gamma} = -4.30$, $D_1 = 0.580$, $D_2 = -1.01$, $L_0 = 20.1$, $L = 22.0$, $\Delta = 1.48$, $\alpha = 1.36$. (D_1 and D_2 are defined in Sec. IV C.) The negative $\hat{\Gamma}$ causes the Argand-diagram resonance circle (for $l < 22$) to curve "backwards."

Regarding the occurrence of spurious fits to angular distributions, they appear to be rather unlikely if the model is capable of providing a sufficiently good fit. Nonunitary fits [i.e., fits which have $\eta(l) > 1$ over some l range] complicated the location of the (poor but unitary) 18-MeV fit, and an excellent but nonunitary fit to the 20-MeV data evidently had such a deep χ^2 minimum that the search routine was incapable of locating an acceptable unitary one. At all higher energies any reasonable starting parameters enabled the routine to find what was apparently the correct fit immediately. The smoothness of the energy dependence of the best-fit parameters is the best empirical test of their consistency, and Fig. 8 shows that,

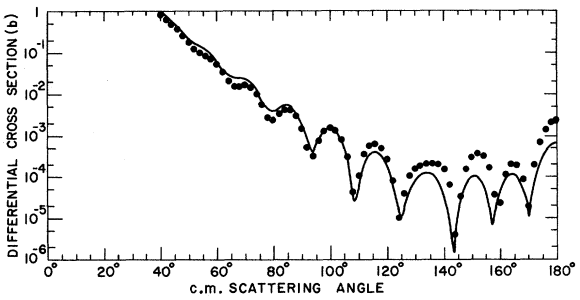

FIG. 10. Two-pole fit to the 18-MeV synthetic data of Fig. 6. The model parameters are $\hat{\Gamma} = 2.39$, $D_1 = 0.0454$, $D_2 = 0.127$, $L_0 = 12.7$, $L = 11.8$, $\Delta = 0.611$, $\alpha = 1.24$; for the second pole, $\hat{\Gamma} = 0.164$, $D = 0.177$, $L_0 = 10.1$.

except for the 22-MeV case, the energy dependence is not only smooth but nearly linear. Incidentally, it is worth noting from the plot of L_0 vs $E_{c.m.}$ that the $n=0$ state moves up two units in l approximately every 4 MeV in this energy range, a point of some interest because the spacing between maxima in the $^{16}O+^{16}O$ excitation function at 90° is not far from 4 MeV.[6]

A slip of the keypunch did turn up one particularly interesting spurious but unitary fit, however. A mis-punched card started out a 32-MeV search with a negative total width, and the routine located the very acceptable fit shown in Fig. 9. Although untenable as a Regge fit because of its negative width (corresponding to a state which grows rather than decays in time), it is unitary and perfectly

TABLE II. Model parameters corresponding to the $\alpha+^{16}O$ fits shown in Fig. 11.

$E_{c.m.}$ (MeV)	$\hat{\Gamma}$	D_1	D_2	L_0	L	Δ	α
20.3	2.86	3.63	1.13	6.45	6.48	0.868	−0.0683
23.0	0.800	1.00	1.00	7.54	8.22	1.00	0.246

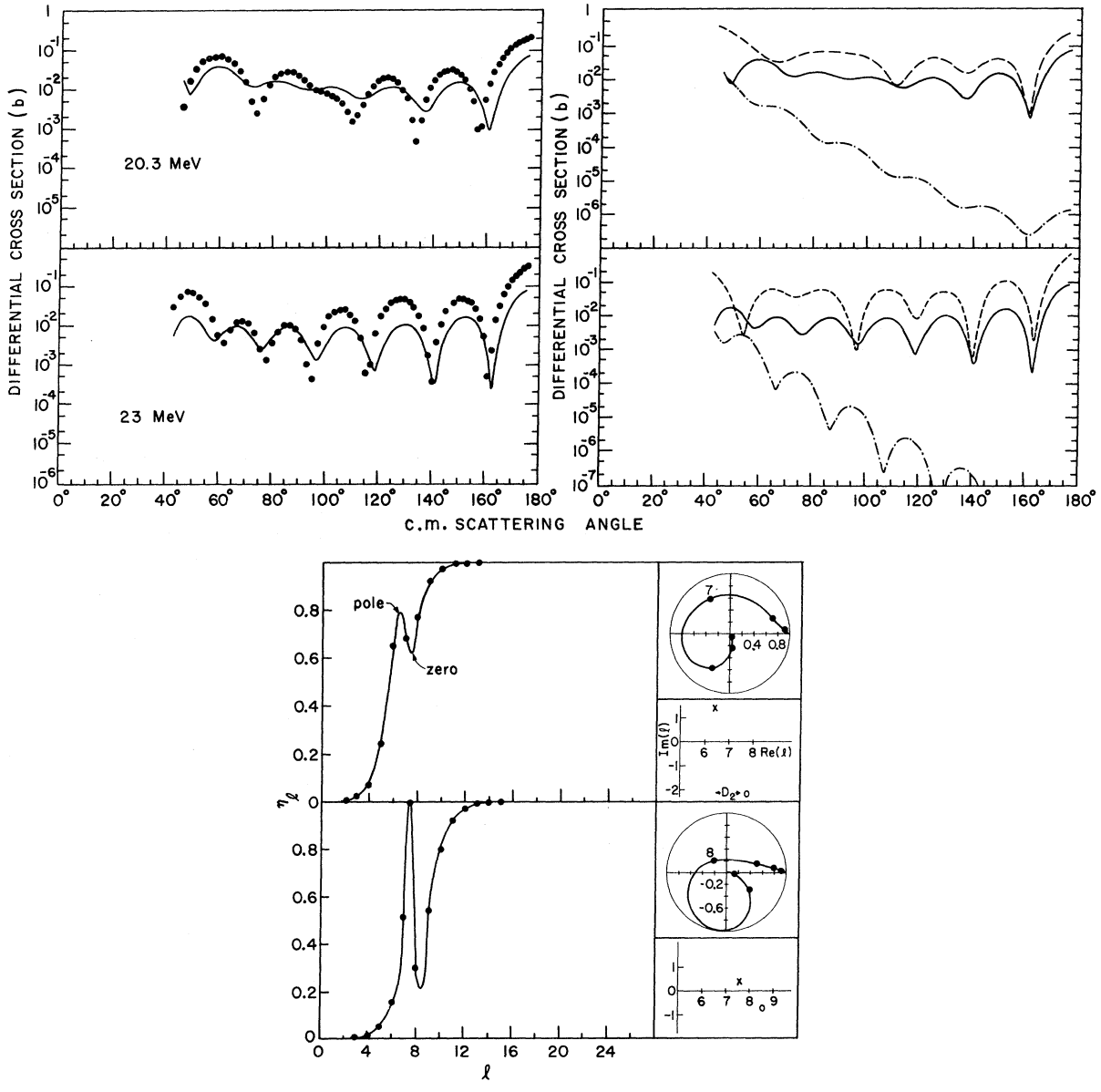

FIG. 11. Seven-parameter model fits to $\alpha+^{16}O$ elastic angular distributions, together with pole-plus-background decompositions as in Fig. 7, and partial wave decompositions as in Fig. 6. The model parameters are given in Table II.

reasonable outside this model. It is particularly interesting in the heavy-ion context because its Argand diagram is very similar to ones which result from the l-dependent absorption model of the Florida State group.[8] Although we have not pursued the matter further, this could suggest that at least some heavy-ion angular distributions can be fit equally well with both models. If so, presumably the smoothness of the energy dependences of the parameters is the only criterion which could be used to decide between them.

C. Extensions of the Model

The model can, if desired, be extended to cover a wider range of physical situations. The following seem to be the most physical ways of adding further parameters:

(1) More poles. Additional pole-zero factors of the same form as that in Eq. (5) can be added at will and should extend the usefulness of the model to lower energies. For instance, a much better fit to the 18-MeV synthetic angular distribution was achieved with two poles, and is shown in Fig. 10. It is somewhat suspect, however, in that its fit to the S matrix elements does not seem to be better than that achieved with one pole.

(2) Phase of the resonance term, or complex D. As in the customary Breit-Wigner approximation in energy, if the resonance is superimposed on a nonelastic background [$|B(l_0)|<1$], it can carry an additional phase, which is equivalent to making D complex, $D=D_1+iD_2$. This moves the zero position to $L_0+iz=L_0+D_2+i(p-D_1)$, which shifts its real part relative to that of the pole L_0 by D_2; for single-cluster Regge poles D_2 is most likely to be positive, putting the zero to the right of the pole.

(3) Better background phase. There is no fundamental reason for introducing the background phase through the $e^{i\alpha}$ factor of Eq. (5), and if it proves inadequate, a more physically motivated l dependence for this phase should be employed.

D. $\alpha+{}^{16}$O Scattering

It is not our intention to investigate α-particle scattering in any detail, but in order to provide some estimate of the applicability of the present model to this process, we have attempted to fit two angular distributions for elastic $\alpha+{}^{16}$O scattering. The data most readily available to us were those of Bergman and Hobbie,[26] in the laboratory energy range 19–23 MeV.

We were unable to obtain unitary fits with the six-parameter model of Eq. (5). The difficulty was very similar to that encountered by Cowley and Heymann[5] in their analysis of the same process at 25–32 MeV: The search routine insisted on adding a "Gruhn-Wall spike," rather than a dip, to $\eta(l)$, corresponding to a rapid resonant excursion of $S(l)$ outside the unit circle. Consequently we extended the model to seven parameters (as in the Cowley-Heymann form) by allowing D to be complex. Because this puts the pole at one l and the zero at another, it adds both a spike (at the pole) and a dip (at the zero). It was then possible to find broad, rather flat-bottomed χ^2 minima which were either within or very near the unitary region of the parameter space, and so locate the unitary fits shown in Fig. 11; the model parameters are given in Table II. Although comparable in quality to the Cowley-Heymann fits, and substantially better than smooth-cutoffs fits, they are not as convincing as the above fits to the heavy-ion optical-potential cross sections. This is not entirely surprising at energies this low, for the Bergman-Hobbie excitation functions show considerable compound-nucleus structure, which one would not expect the present model to fit any better than the smooth-cutoff model would.[27] Substantially better fits should be obtainable at higher energies. Analyzing the fits into pole-plus-background contributions shows them, again, to be very dependent on interference between the two.

V. CONCLUSION

Regge poles are found to provide a very convenient means of understanding the partial-wave decomposition of optical-potential amplitudes in the resonant energy range. Even if the potential is so absorptive that it exhibits no visible resonances, the smooth-cutoff behavior of its scattering amplitude is understandable in terms of many overlapping inelastic Regge resonances. In the special case that the potential is strongly absorptive near its center but fairly transparent near its edge it may support nonoverlapping resonances only for l values near $l=kR$ and so be describable in terms of a single Regge pole there, together with strong absorption at smaller l's.

This distinctly appears to be the case for an optical potential used by the Yale-Argonne group[20] to describe ${}^{16}\text{O}+{}^{16}\text{O}$ scattering, and a brief examination of some elastic $\alpha+{}^{16}$O data lends support to the suggestion of Cowley and Heymann[5] that a one-pole model may be applicable to this system as well.

Although we have employed optical (i.e., pure single-particle) resonances as a convenient nuclear example of direct-channel Regge poles, this should not be taken to imply that the Regge parametrization is restricted to optical resonances, nor that optical resonances are the only possible manifestation of Regge effects in nuclear reactions.

Resonances which are predominantly but not totally single particle are, in fact, far more likely to occur.[28] Being narrower (because of their closed-channel components) they cannot be described by an optical potential but should be quite adequately described by the parametrization suggested here.[29]

Perhaps the most distinctive characteristic of a single-pole-plus-background angular distribution (visible only if the full angular range is available) is its "two-slope" character. Averaging through the angular oscillations, it falls steeply at forward angles where the background-plus-Coulomb effect is dominant, and switches to a lower slope at backward angles where the Regge pole or glory effect dominates. Deep diffractionlike minima typically occur at the break in the slope, often separated from the backward-angle oscillations by a characteristic "smooth section," as shown in Fig. 6.

ACKNOWLEDGMENTS

It is a distinct pleasure to acknowledge many fruitful discussions with R. H. Siemssen, whose data and enthusiasm for the subject provided the major stimulation for this investigation. Many helpful suggestions were also offered by C. J. Goebel, H. T. Richards, L. A. Sromovsky, J. V. Maher, and W. A. Romo. Invaluable assistance with the computations was graciously extended by C. M. Vincent, S. Cohen, P. L. Jolivette, and M. Menzel. In this regard special thanks are due S. Cohen for making available the interacting console terminal of the Argonne National Laboratory 360/75 computer; this terminal, combined with Cohen's SPEAKEASY language, facilitated a data-fitting procedure which would otherwise have been extremely difficult if not impossible. Finally, it is a pleasure to thank M. Peshkin for the friendly hospitality extended by the Argonne National Laboratory, where much of the work was done.

Note added in proof: We wish to thank Singh[30] for calling our attention to elastic angular distributions for α particles on ^{24}Mg which at 80 MeV exhibit a remarkable example of the "smooth section" seen in Fig. 6 of the present work.

---

*Work supported in part by the U. S. Atomic Energy Commission and the National Science Foundation.

†Home address: Department of Physics, University of Wisconsin, Madison, Wisconsin 53706; on leave, 1970–1971, Department of Physics, Brooklyn College, Brooklyn, New York 11210.

[1]J. S. Blair, in *Lectures in Theoretical Physics*, edited by P. D. Kunz and W. E. Brittin (University of Colorado Press, Boulder, Colorado, 1966), Vol. VIII, p. 343; W. E. Frahn, in *Fundamentals in Nuclear Theory*, edited by A. deShalit and C. Villi (International Atomic Energy Agency, Vienna, Austria, 1967), p. 3.

[2]H. C. Bryant and N. Jarmie, Ann. Phys. (N.Y.) 47, 127 (1968).

[3]A detailed account of the relation between the glory effect and surface Regge poles can be found in L. A. Sromovsky, Ph.D. thesis, University of Wisconsin, 1970 (unpublished).

[4]C. R. Gruhn and N. S. Wall, Nucl. Phys. 81, 161 (1966).

[5]A. A. Cowley and G. Heymann, Nucl. Phys. A146, 465 (1970).

[6]J. V. Maher, M. W. Sachs, R. H. Siemssen, A. Weidinger, and D. A. Bromley, Phys. Rev. 188, 1665 (1969).

[7]R. H. Siemssen, H. T. Fortune, R. Malmin, A. Richter, J. W. Tippie, and P. P. Singh, Phys. Rev. Letters 25, 536 (1970).

[8]R. A. Chatwin, J. S. Eck, D. Robson, and A. Richter, Phys. Rev. C 1, 795 (1970).

[9]H.-D. Helb, H. Voit, G. Ischenko, and W. Reichardt, Phys. Rev. Letters 23, 176 (1969).

[10]The inclusion of the phase α in the denominator is merely a convenient device, suggested by T. E. O. Ericson [*Preludes in Theoretical Physics*, edited by A. deShalit, L. Van Hove, and H. Feshbach (North-Holland Publishing Company, Amsterdam, The Netherlands, 1965), p. 321], for providing S_l with a reasonable phase for l near L. $\alpha > 0$ gives S_l a positive phase, and if $-\pi/2 \leq \alpha \leq \pi/2$, then $|S_l| \leq 1$.

[11]$D(l) = p(l) - z(l)$ is approximately the distance (in l) between the zero and pole of this expression in the l-plane. The elastic width of the resonance is given approximately, for narrow resonances, by $|B(l_0)|D(l_0)$. Note that *both* the elastic and total width must be l dependent.

[12]N. Austern, Ann. Phys. (N.Y.) 15, 299 (1961).

[13]As explained below, these maxima are actually associated more closely with the zeros of $S(l, E)$ than with its poles, but the two always occur in associated pairs.

[14]These are the transmission coefficients for essentially the 17-MeV potential employed by Maher *et al.* (Ref. 6) to describe ^{16}O–^{16}O scattering, modified by holding its (volume) imaginary well depth fixed at 0.5 MeV.

[15]This can be seen most concisely by using Regge's expression for $\partial E_{n,l}/\partial l$: $\partial E_{n,l}/\partial l = (2l+1)\hbar^2\langle 1/2\mu r^2\rangle$, where the expectation value is with respect to the wave function of the (n, l) level. Since $\langle r^{-2}\rangle > R^{-2}$, where R is the radius of the potential, $\partial E_{n,l}/\partial l > (2l+1)\hbar^2/2\mu R^2$, and the right-hand side of this expression is just the rate at which the barrier height increases with l.

[16]The central role played by the Regge zero is our main reason for employing the pole-zero representation of Eq. (4), which *multiplies* $B(l)$ by a pole factor, rather than that of Cowley and Heymann (Ref. 5), which *adds* a pole to $B(l)$. The multiplicative form has the advantage of including the zero position explicitly. The additive form must, of course, also have a complex zero, but it would

not be simple to locate, and may not even occur near its "correct" position, because of the unphysical behavior of the Woods-Saxon $B(l)$ for complex l.

[17]An optical potential manages this much more subtly, using an infinite number of fixed poles rather than a few moving ones. In the best "duality" tradition its $S(l)$ has poles where it needs them, at low l, while simultaneously preserving the correct asymptotic exponential behavior as $l \to +\infty$. A simple example of how this can be done with an infinite number of poles is seen in the familiar infinite-product representation for the cosh function: $(e^z+e^{-z})^{-1}=\frac{1}{2}\prod_{n=0}^{\infty}[1+4z^2/(2n+1)^2\pi^2]^{-1}$. It has poles for $z=\pm i(2n+1)\pi/2$ for all integral n, as Ericson (Ref. 10) has noted in his Regge representation of the smooth-cutoff model itself. Since these poles have also been employed by E. V. Inopin {Zh. Eksperim. i Teor. Fiz. 48, 1620 (1965) [transl.: Soviet Phys.-JETP 21, 1090 (1965)]} and J. Högaasen [Nucl. Phys. A90, 261 (1967)], it is perhaps worth remarking that they should be thought of merely as a mathematical device—useful but without physical significance. Although the Fermi function provides a very reasonable representation of the smooth cutoff for real l, its behavior at complex l values is entirely unphysical. Its poles lie along a vertical line in the l plane, unlike those of any physical amplitude, and in a configuration which could never describe an $\eta(l)$ curve with several minima.

[18]N. N. Khuri, Phys. Rev. 130 429 (1963); E. Jones, Lawrence Radiation Laboratory Report No. UCRL-10700, 1963 (unpublished).

[19]U. C. Voos, W. von Oertzen, and R. Bock, Nucl. Phys. A135, 207 (1969).

[20]J. V. Maher, R. H. Siemssen, M. Sachs, A. Weidinger, and D. A. Bromley, in Proceedings of the Heidelberg International Conference on Heavy Ions, Heidelberg, July, 1969 (to be published).

[21]We are grateful to Dr. J. V. Maher and Dr. R. H. Siemssen for suggesting this potential as appropriate for the purpose, and for providing its parameters prior to publication. We should remark that although the angular distributions of this potential are nearly identical to those of their original potential (see Ref. 6) when the amplitudes are symmetrized, the two are quite different when not symmetrized. The present model was incapable of fitting the cross sections of the original more transparent potential, because it has several "active" Regge poles while the model has only one.

[22]The background and resonant "contributions" to the partial-wave amplitudes are multiplicative rather than additive in this case, so the traditional interference terminology is not entirely applicable, but clearly the same type of effect is involved.

[23]More accurately, a one-modified-pole phenomenon, since without the l-dependent widths the average slope of the angular distribution would be much steeper.

[24]Even though the magnitude of the scattering amplitude does not oscillate across the smooth section, its real and imaginary parts do, 90° out of phase, with an angular period slightly greater than that of the forward and backward oscillations.

[25]The values obtained at $E=22$ MeV are slightly anomalous, so the trajectories are not drawn through them. If the potential were real, the pole and zero trajectories would be symmetric about the real l axis; to a first approximation they are simply displaced vertically by making the potential complex.

[26]C. Bergman and R. K. Hobbie, Annual Report of the J. H. Williams Laboratory of the University of Minnesota, 1968 (unpublished), p. 21, and to be published. We are grateful to H. T. Richards for bringing these data to our attention, and to R. K. Hobbie for making it available before publication.

[27]At individual resonances which are not correlated in l the more customary smooth-cutoff model plus Breit-Wigner resonances (in energy) would seem more appropriate, such as that used by M. K. Mehta, W. E. Hunt, and R. H. Davis, Phys. Rev. 160, 791 (1967).

[28]One such example has recently been suggested by W. Scheid, W. Greiner, and R. Lemmer, Phys. Rev. Letters 25, 176 (1970), who consider the possibility that while the two nuclei are trapped in a single-particle or quasimolecular state, they may individually be raised to (bound) states of internal excitation, thus "locking up" some of the energy available for relative motion. The resulting resonance state will be a mixture of resonant and bound (closed-channel) states which obviously have a longer lifetime and hence a narrower width than the pure single-particle state.

[29]Because the effects of these surfaces resonances are largest at backward angles, where elastic nucleon-transfer effects (Ref. 19) are also most prominant, the problem of distinguishing between the two is likely to be of paramount importance. Consequently, it seems worth noting that whenever the reaction proceeds through a resonance (of sufficiently long life), a distinction between direct and exchange scattering neither can nor should be made. Taking the scattering of ^{16}O on ^{12}C as an example, the target and projectile ^{12}C "cores" can in principle be distinguished if the reaction is "direct" (prompt) by the fact that it is the projectile core which proceeds in the *forward* direction throughout the reaction. In this case, as W. von Oertzen has argued [Nucl. Phys. A148, 529 (1970)], any exchange amplitude present must be added to the direct (e.g., optical-model) amplitude. If, however, the reaction is resonant, the distinction between the two cores is lost in the intermediate state. Direct and exchange contributions are no longer distinct in this case and consequently it would appear to be incorrect to add an exchange contribution to a resonant "direct" amplitude. In this light, the sawtooth shape of von Oertzen's $\eta(l)$ curve for ^{16}O and ^{12}C, Fig. 9, which indicates the presence of several Regge resonances, might cast doubt on the validity of his approach in this particular case.

[30]P. P. Singh, R. E. Malmin, M. High, and D. W. Devins, Phys. Rev. Letters 23, 1124 (1969).